University of Thi -Qar Journal for Engineering Sciences
http://www.doi.org/10.31663/tqujes.12.1.418(2022)
Vol 12.1 (April2022)

ISSN :2664- 5572 (online)
ISSN:2664-5564 (print)
Available at http://jeng.utq.edu.iq
utjeng@ utq.edu.iq

Effect of volume fraction on flow properties for centrifugal pumps for mixed flow

Mohammed Saker Talab[†]Asst. prof . Dr . Husam ALI Khalaf[‡]

[†]First author's Mechanical Engineering, College of Engineering, Thi-Qar University, Iraq, MohammedSaker @utq.edu.iq
[‡]Second author's Mechanical Engineering, College of Engineering, Thi-Qar University, Iraq. HusamAli @utq.edu.iq,

Abstract

The performance of a centrifugal pump employing a single-step centrifugal pump under a gas-liquid mix and with a single suction pump is displayed. volume fracture ratios, IGVF % (1,5,10,15) 2compared with the flow rate Q/Qdes,w (8-1,2), the experimental and numerical simulations have been compared. The findings are presented by coefficients without dimensions from the similarity law. The computational results have shown that the nominal rotational velocity of numerous flow parameters has achieved good agreement on the experimental data, with the degradation in the head being noticed step by step, i.e. the bigger the volume ratios, the more the head deterioration is. The coefficient of inflow declines.

Keywords: Effect ,volume fractio,n mixedf low, properties, IGVF, Q/Qdes,w

1. Introduction

The centrifuge pump with a spinning impeller is the rotodynamic pump. A fluid impeller is used to enhance the pressure of a fluid. The fluid is sent into the pump's rotating impeller as a stream. The impeller consists of a rotating disc with several blades known as vanes attached and sometimes reclined in the direction of the rotation. The flow is stopped by the suction impeller when the whirling vanes get near. Mixed flow studies have been undertaken for a long time and both hydraulic performances have so far been improved and internal flow patterns revealed. Based on the unstable inviscid calculations and loss models,**[1]**examined the hydraulic performance of the mixing flow pump. Gas training in an ESP may produce a modest boost pressure deterioration in low GVFs, a severe fall in GVFs at relatively higher levels, and eventual full pressure-boosting loss. The phenomenon, **[2]**have carried out pioneering experimental work on the two-stage performance of centrifugal pumps (1974). With the entraining of increasing gas levels, they noticed hydraulic head degradation and abrupt flow pattern shifts. Multi-stage and inlet impacts from GVF were examined by **[3]**using a two-stage flow loop for ESP increase in pressure. Their work has shown that the GVF inlet is the major factor determining the increase of two-phase pressure in the ESPs. In addition, the ESP increased pressure has been severely degraded in higher GVFs.**[4]** discovered that bubbles grew as intake GVFs increased and rotating speeds were lowered by viewing the internal ESP flow. This expansion reflects the weaker pump performance, which showed that the bubble behavior, in defining the ESP's gas-liquid mixture management capacity, played a major influence. Moreover, Visualization experiments also indicated various flux patterns in higher ESP channels. An additional visualization study has been carried out **[5]**that has taken into account surfactant impacts on the ESP double phase pressure increase. His experimental findings showed that strain can diminish surfactants, hence reducing bubble diameters and deferring the creation of gas pockets to greater GVFs. Using a 14-stage radial-pump, **[6]**examined the two-stage performance of a multi-stage ESP for influences from stage number, intake pressure, gas injection pressure, and fluid. The pressure increase in the ESP was found to vary only step by step with relatively high intakes of GVF. The ESP pressure increase degradation is mild at low GVFs.**[7]**. have carried out a more current visualization work on the quantification of the gas-phase part within a revolving centrifugal pump impeller (2015). The in-situ αG distributions under stable flow conditions were estimated effectively using sophisticated technology HireCT (high-solution gamma-ray computer graphics tomography), with various pump rotational speeds and intake GVFs.Visualization investigations can easily disclose gas-liquid-flow phenomena by directly observing flow patterns inside the ESP impeller. The pump geometry experimental facility needs particular designs, including removal of the hub of the pump and attachment of the Pyrex glass on its top for visualization. [**8**]

also noted that it is considerably harder to visualize two-stage flow topologies in series-built ESP. In the documentary literature, the two-phase gas-liquid flow in the mixed-flow pump is not very open studied and analyzed. This article analyzes in-depth the impact of the gas volume percentage on the two-phase mixed-flow pump flow performance. The results are examined both under the constant proportion of the gas volume and the transient variation procedure. For an optimal design of mixed-flow pumps, the research content may be utilized.

2. GDM 10 x 12 HD Centrifugal Pump

In the present study, the pump model investigated is the Gardner Denver (GD)M 10 x 12 HD (Fig.1). This model represents a radial flow pump in which the working fluid inlet is located at the center of the impeller (rotating part) and fluid outlet at a right angle to the pump shaft located at the volute (Stationary part). However, this type of centrifugal pump referred to be integrated with the ESP systems **[13]**. From the fundamentals of pump components, the impeller work to increase the kinetic energy in the working fluid. However, the volute captures the velocity of fluid flows as it passes in the outermost diameter of an impeller and converts the velocity to pressure. These two main parts were illustrated in Fig.1.

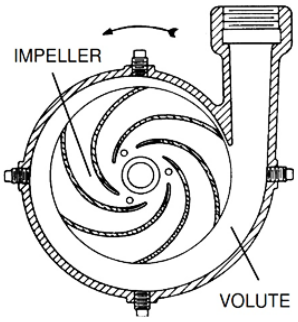

Fig.1 convergence graphical windows appears.

2.1 Validation

The GDM 10 x 12 HD pump model has been validated **[13]**. At the operational state, model validation was performed for a single-phase water flow and base pump model specification.

2.2 Physical Model

For validation reasons, the computational analysis was assumed to be steady-state. The simulation has two physical domains: impeller (rotor portion) and volute (stationary part). Water is used as a working fluid, and the fluid flow is described as incompressible flow. In addition, the k-model was employed to solve turbulence characteristics.

3. The initialization

For each case run, the system was analyzed at the beginning with steady-state simulation. Then results are used toCalculate the starting value for transient solutions.
In Ansys CFX, initialization is accomplished by entering starting guess values for the governing equation so that the flow field variable can be approximated and solved by iteration toward the solution.
Radial pumps are typically utilized in ESP systems that need a high head installation.The pump in question has a rotating velocity of 800 to 2000 rpm and a nominal flow rate of less than 1135.62 m3/hr **[14]**. The key characteristic of this pump is its segmented architecture, which makes it simple to maintain.
Vertical and horizontal positioning is also possible thanks to a robust steel frame with an increasing bracket. Table 1 summarizes the design characteristics of the investigated pump.**[13].**The cases were investigated for hydraulic performance and compared with the crude oil single-phase results.

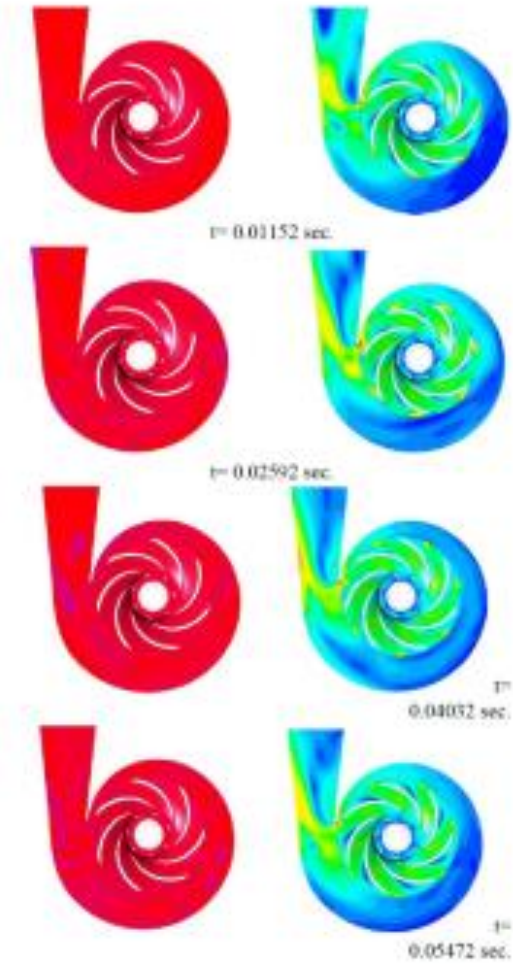

Fig.2considered for the case of 5% gas volume fraction.

Results of each working condition were captured after achieving stable data in the last period of transient calculation. It can be observed in the Fig.2 that the hydraulic head of the centrifugal pump is decreased with the increase of IGVF.

3.1 Work on experiments

investigated radial stage configuration alterations using high-speed imaging**[9]**. To decrease the gas effect on the head of the pump. They noticed that the gas was accumulated by the impeller blades on the suction line. There was a gas pocket holding the For low gas flow rates at the impeller outlet and progressing toward the inlet when the inlet is with the rising gas fraction, efficiency deteriorated. They, based on these findings, To prevent gas accumulation, he gave some analytical architecture recommendations

1. To prevent gas accumulation by leakage, leave the impeller tip open.
2. Using a diffuser with vanes that are near to the outlet of the impeller.
3. Hold the angle high for the impeller outlet blade.

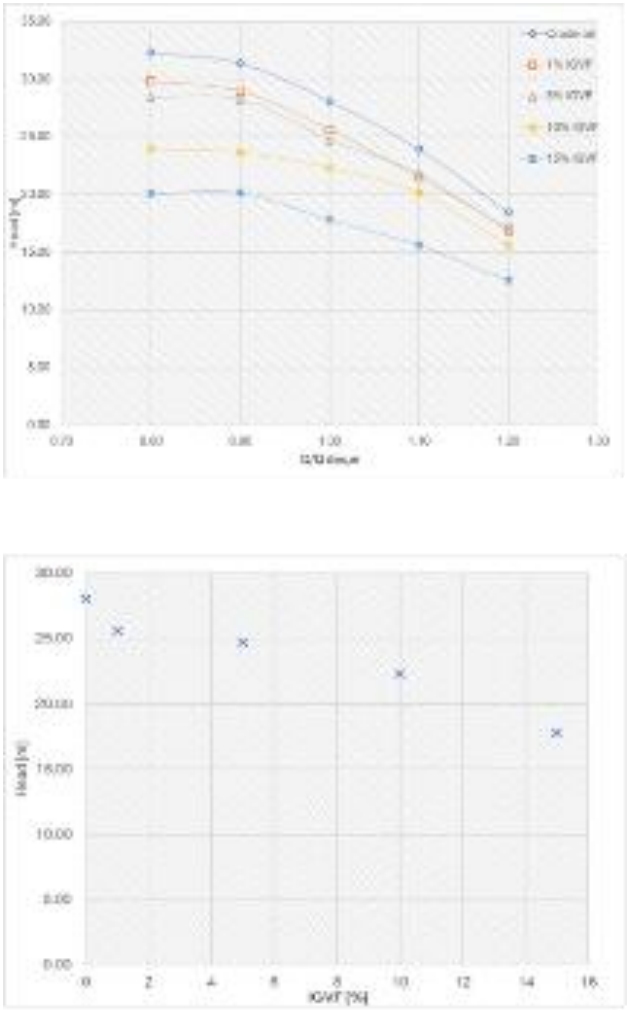

Fig.3 head and Q/Qdes.

4. Breaking up gas bubbles in the impeller with recirculation hol Several flow patterns exist in a singlepattern, according**[10]**. The gas bubbles were always spherical but ellipsoidal, according to the radial impeller. Gas bubbles accumulated in the surrounding river on the pressure line, consolidated and recirculated under surging conditions (about 0.3 percent gas volume fraction in their instance). Although a gas pocket occurs at the suction line impeller input, the impeller outlet does not. The gas pocket increased until the entire channel was blocked, resulting in the activation of a "gas lock. As a result, it's critical to investigate and disclose the internal flow dynamics of centrifugal pumps when they're subjected to gas entrainment. Several ground-breaking investigations on foundational theory, computational modeling There has been researching and testing on how gas entrainment impacts pump efficiency**[2]**carried out research and published a report. Model of two-phase, one-dimensional flow. When they added extra air to the system, they noticed hydraulic head loss and unanticipated flow pattern variances**[9]**. used a tandem blade sequence with an outlet impeller blade angle greater than 90 degrees. The gas pooled in the recirculation zones, according to**[10]**, who performed computational single-phase simulations using the same pump architecture. It appeared to be the source of

recirculation, which had already been observed in single-phase activity. **[8]**studied gas dispersion in a veiled centrifugal radial impeller using Gamma-Ray tomography. The fraction of gas volume that has been averaged across time is alpha1. The incoming gas cut (λ) was still much higher, indicating a severe discontinuity. When (λ 0) increased from (3 to 3.3 %), the local gas volume increased from (24 to 48 %) at a vital gas fraction (λ 0 = 3%). They had noticed that the gas pool had reached its capacity. In the pump's input area, the gas had accumulated. They, along
experts in the field [9] (1996), The passage investigated the impact of a balance hole drilled in the hub, and discovered that the gas concentration was reduced where the hole was drilled **[11]**. They produced a lot of output in two-phase flow, but the architecture didn't work well at low flow rates. Using the inner wall of the diffuser of a three-stage Multi-Vane Pump, impellers with open blades **[12]** computed the fraction of the in-situ gas volume (MVP, marketed by Centrilift). There was a considerable difference, as demonstrated by these measurements. These parameters provided a general distinction between the gas cut and the fraction of local gas (λ < a).

4. System Analysis Stationary

[26]has been utilized to calculate an ESP operation point for the steady-state systems analysis. This method is also known as the nodal analysis to compute the sequential pressure drops to be overcome by the produced fluid.
First, the manufactured fluid is dumped into the well from the tank. At this point, The Darcy equation regulates pressure losses. The connection between Flow rate Q and drawdown (Pres −Pbh) are so-known as productivity

Q=P(Pres-Pbh) (1)

The lower pressure hole is Pbh, while the mean static pressure reservoir is Pres. Assume a single-phase incompressible flow that is homogeneous, radial, and homogeneous.
The reservoir would be constant and the Productivity Index Properties storage tank would be fluid-dependent. Theoretical link between the foundation and the base. under constant tank pressure, hole pressure and fluid flow (100 percent water: The straight line has been dashed).The petroleum bubble point may also be below more precise models for oil and water production fluid pressure. Different cuts are available (water flow rate to total flow rate) water cutbacks of varying degrees The Composite Inflow Relationship Curve is a graph that represents the relationship between inflow and out (IPR), The pressure at the bottom of a well is equal to the pressure of a sand face bottom hollow (SBHP) when no liquid flows.The reservoir begins to flow as the underlying loop pressure is reduced, however when the bubble point pressure is reached, the gas is liberated from the solution, and the Q-rate differs from that of the linear model. It is possible to obtain a maximum flow of 0% water. The second gradient to be overcome by the pressure from the container to the well's head is the hydrostatic stress of PH, which is proportional to height H. That word is straightforward if you know the density of the fluid you've made.

ΔP = ρ g H (2)

Finally, friction via the tubes and choke is most likely a quadratic flow rate function, with the friction coefficient Cf based on position, tube diameter, roughness, and fluid physical properties

ΔPf (d.Q)=ρC f (d.ϵ) Q2 (3)

The electrical dip pump adjusts the pressure increments in accordance with the P pump speed or frequency f (= 2 ff) and the total Qtot flow rate. The pump OpenType equation is used in this case. ed. Head Hpump is a frequent sign of increased pressure.

Δ**P**pump(□,Q)=**P***g*H pump (f,Q) (4)

If the reservoir pressure is constant, the pump discharge pressure from the reservoir to and from the surface is computed as follows:

⌈Pd=Pbh+ΔPpump= Pbh+ ρ*g* Hpump
Pd =Pωh +ΔPf +ΔPh= Pωh+ ρ Cf (d,**ϵ**) Q2+ρ*g*Ĥ] (5)

The pump operating point is defined by these two equations:
(f, Q)= 1

The junction of the system can also be graphically resolved "pump curve" (left hand) and "system curve" well performance curve (right) hand side). Fig3.2 shows them for various pump speeds And the sizes of the tubes. Each crossroads symbolizes a possible place of operation.

Hpump(□,Q)=1/(ρg)(Pωh– Pbh+ρ Cf (d,**ϵ**) Q2) + Ĥ (6)

Single phase ESP head curves and system curves The solid lines designated by the pumping speeds represent the pump head curves for one specific pump at various speeds. Better efficiency point (BEP) is represented by fractured lines, and greater operating range is represented by lower operating range. Two different sizes of tubes are represented by the two "well-performance curves." (different friction loss coefficients) The operating point is close if the system is the right size. The Best Efficiency Point (MBEP) pump, or at the very least within the operational range.

H=(PSTATIC,OUT–PSTATIC,IN.)/(ρg) (7)
η=ρgQH/ M***ω***(8)

For a single-phase system, the ESP head curves and system curves The pump head curves are represented as solid lines enumerated with pump speeds for a given pump at various speeds. The dashed lines correspond to the lower operating range, the Best Efficiency Point (BEP),

and the wider operating range, respectively. Two different tube sizes (or system curves) are depicted in two "excellent efficiency curves" (different friction loss coefficients). The operating point is near to, or at least within, the pump's working range, thanks to proper system sizing. Point of Maximum Efficiency.

4.1 The Mathematical Model

Unsteady Reynolds-Averaged Navier-Stokes Equations (U-RANS) are mass and momentum equations that can be expressed in a generic form as;where ρ is the fluid density and $\vec{V}$ represents the:

$$\rho\frac{\partial\Phi}{\partial t}+\nabla\bullet(\bar{\nabla}\Phi)=\nabla\bullet(\Gamma\nabla\Phi)+S \quad (9)$$

$\Phi=1$

$\Gamma=S=0$

$\Phi=\bar{\nabla}$ Reynolds-averaged velocity vector relative to the frame of

being seen as a reference The continuity equation makes the following assumptions:
In the case of momentum equations,

$\Gamma=\mu+\mu_t$

And

$$S = -\nabla P + S_{cor} + S_{cfg} \quad (10)$$

where μis the fluid dynamic viscosity, t is the turbulent or eddy viscosity calculated using Reynolds averaging and the Boussinesq hypothesis, and p is the pressure gradient S_{cor} and Scfg, on the other hand, represent the Coriolis and centrifugal influences, respectively.
Due to turbulence, The standard k-ε transport equations obtained for turbulence kinetic energy, k, and its dissipation ε are given by the following equations respectively.
For turbulent kinetic energy k,

$$\partial(\rho\kappa)/\partial t+\partial/\partial x(\rho UjK)=\partial/\partial xj\ [(\mu+\mu t/\sigma\kappa)+\partial\kappa/\partial xj]+P-\rho\varepsilon+P\kappa b \quad (11)$$

For turbulence dissipation ε,

$$(\partial(\rho\varepsilon))/\partial t+\partial/\partial xj(\rho Uj\varepsilon)=\partial/\partial xj[(\mu+\mu t/\sigma\epsilon)\partial\varepsilon/\partial xj]+\varepsilon/\kappa\ (C\varepsilon_1\ P\kappa-C\varepsilon_2\rho\epsilon+C\varepsilon_1\ P\epsilon b) \quad (12)$$

Pkb and Pb denote the effect of buoyant forces, while Pk denotes the turbulence produced by viscous forces. C1 = 1.44, C2 = 1.92, C = 0.09, = 1.3, and k = 1. The model constants are C1 = 1.44, C2 = 1.92, C = 0.09, = 1.3, and k = 1. **[21].**

- Boundary Conditions

The mass flow rate at the computational domain's entrance is specified as 0.251 m3/s (903.6 m3/h). Pressure is imposed at the outlet in accordance with the operating state (Total pressure = 1 am). A no-slip flow condition is also applied to the walls (on the blade, hub, and shroud). Because of the difference in reference frames between the static volute and the revolving impeller, the impeller-volute interaction was modeled using the Frozen-Rotor interface model. Finally, the impeller's rotational speed was set to 1400 rpm.

4.1.1 Buoyancy in Multiphase Flow

In addition to the buoyancy forces that can exist in single-
In multiphase flows, the difference in density between phases creates a buoyancy force (including particle tracking). As a result, in multiphase flows, buoyancy is virtually always relevant. It's crucial to get the buoyancy reference density right for multiphase flows. The buoyancy reference density for a flow with a continuous phase and a scattered phase should be set to the continuous phase. The reference density of the continuous phase wipes out buoyancy and pressure gradients in the momentum equation because the pressure gradient is practically hydrostatic for buoyant.
The Boussinesq model is employed. For all factors other than the buoyancy source term, a constant reference density ref is employed in this model. **[27]** is a rough approximation of the buoyancy source term.

$$p-\rho=-\rho ref\beta(T-Tref) \quad (13)$$

$$\beta=-1/(\rho)\partial/\partial\rho/T\ |P \quad (14)$$

Where β is the thermal expansivity;

4.1.2 Multiphase Flow with Homogeneity

Homogeneous multiphase flow is a limiting situation of Eulerian-Eulerian multiphase flow in which all fluids have the same velocity fields and other relevant fields like temperature, turbulence, and so on. All fluids have a common pressure field.

4.2 Model of Eulerian-Eulerian

The Free Surface Simulate can be used to model certain interphase transfer terms utilized in momentum, heat, and other interphase transfer models inside the Eulerian-Eulerian model.Summing the multiple phasic transport equations over all phases yields a single bulk transport equation for **[27]:**

$$\partial/\partial t(\rho\Phi)+\nabla\bullet(\rho U\Phi-\Gamma\nabla\Phi)=\mathbf{S} \quad (15)$$

$\Gamma=\sum_{a=1}^{Np}[\![a\Gamma a]\!]$ U1/ρ

$\sum_{a=1}^{Np}[\![a\rho aU]\!]$ aere

$\rho=\sum_{a=1}^{Np}[\![\Gamma a\rho a]\!]$

the continuity equation and momentum equation is expressed as follows:

$$\partial/\partial t(ai\rho i)+\nabla\bullet(ai\rho i\omega i)=O \quad (16)$$

$\partial/\partial t(a_i\rho_i\omega_i)+\nabla.(a_i\rho_i\omega_i\square\omega_i)=-a_i\nabla\rho_i+\nabla\bullet(a_i\mu_i(\nabla\omega_i+〚(\nabla\omega_i)〛\hat{}T))+M_i+a_i\rho_i f_i$ (17)

In the formula, i- any phase (l for liquid;g for gas)
pi i phase pressure
ai the volume fraction of i phase
ρ i i phase density Ai
Mi the interphase force exrted on i phase
ωi i ralative velocity of i phase
f i mass force of i phase related to impeller rototion
μi i phase dynamic viscosity
H Head
Q Mass flow rate
GVF inlet gas volumetric fraction
Ƞ Efficiency
BEP best efficiency point
ΔP stage pressure incrementPa
N phase number
NP normalized pressure increment
R representative radius, L, mm
RS dimensionless notation
Re Reynolds number
Sr Strouhal number
α gas void fraction
β tangential blade angle
λG no-slip gas void fraction
μ molecular viscosity
μt turbulent viscosity
μeff effective viscosity
Ω rotational speed
Hirect high solution gamma ray graphics tomography.

5. Conclusions

The effect of gas volume on the flow characteristic of a mixed pump is shown in this article Methods for experiments have been studied. Both findings are below the Constant proportion of the gas volume and transit gasThe quantity change procedure is compared. Comparison of the factory and volume fraction observed The process of changing the quantity is compared. Observed when comparing factory and volume fraction.
(1, 5, 10, 15) % IGVF
1- The deterioration of the head according to the different percentages, and the deterioration was gradual along with the flow rate Q/Qdes, w = (8-1,2) and the percentages of deterioration against each of them:
- at 1% 25.5639 %
- at 5% 29.0076 %
- at 10% 43.9024%
At 15% 60. 8646 %
2- It was observed that the pump power increased at the same values of the flow rate and the aforementioned volume fractions at Q/Qdes,w = 1.1 for the factory and the other volume fractions.
- at 1% 11.4286%
- At 5% 15.2727%
- at 10% 17.6471%
- at 15% 20.8955%

Through numerical study and simulation, the head deteriorates as the volume fractions increase and the pump efficiency decreases Due to a clear density of blade asymmetrical vapor. The cavities are produced and usually develop on the suction side of the blade below every cavity case.The gas input has about the same effect as Blade pressure direction, however pressure amplitudes of the blade surface varied. The interaction of the rotor and the stator is primarily determined. According to the transient pressure oscillation characteristics,

Generally, the radial pumps are used in ESP systems where a high head installation is required. The considered pump has a rotating velocity ranged from 800 rpm to 2000 rpm and a nominal rate of range less than 1135.62 m3/hr **[14].** The main feature of this pump is that it has a segmented construction that is easy to maintenance. Also, a heavy steel frame with the escalating bracket allows for vertical and horizontal positioning. Design parameters of the studied pump are summarized in Table 1 **[13].**

Table 1 main parameters of the pumb.

Impeller characteristics	
Flow rate	0.251 m^3/s
Head	42.6 m
Rotating speed	1400 RPM
efficiency	61%
Inlet diameter	255.7 mm
Outlet diameter	430.6 mm
Hub diameter	77.2 mm
Inlet angle	20.1°
Outlet angle	14.1°
Blade thickness	12.9 mm
Blade number	7
Outlet width	60.5 mm
Volute specifications	
Inlet width	114.3 mm
Cutwater clearance	23.5 mm

Cutwater thickness	9 mm
Exit hydrodynamic diameter	215.1 mm

These performance parameters are taken by **[13]** equivalent to those in the manufacturer data **[21]** as we will show later invalidation section.

Table 3 All simulation conditions are summarized

Case	Working Fluid	IGVF	N (rpm)	$Q/Q_{des,w}$	blades number
1	Crude oil+ Propane gas	1%	1400	0.8 0.9 1 1.1 1.2	7
2	Crude oil+ Propane gas	5%	1400	0.8 0.9 1 1.1 1.2	7
3	Crude oil+ Propane gas	10%	1400	0.8 0.9 1 1.1 1.2	7
4	Crude oil+ Propane gas	15%	1400	0.8 0.9 1 1.1 1.2	7

Thermodynamic properties of crude oil and propane gas:
The physical and thermal properties of the crude oil are presented in the Tables below. The properties considered were considered due to several related references which are **[13],[14],** and **[16]**.

Table 2 cruid oil and propane gas.

	Density [kg/m^3]	Thermal conductivity [W/m.K]	Specific heat [kJ/kg.C]	Dynamic viscosity [kg/m.s]
Crude oil	823	0.0738	2.072466	0.0025
Propane gas	20.592	0.019985	1.9845	$8.556*10^{-6}$

Study Cases
Various Inlet Gas Volume Fractions (IGVF)

In this study, investigations for four IGVF on oil-gas flow have been done. The analysis setting was utilized to achieve a solution. In addition, the mesh of 1,436,555 elements was chosen to be used in all simulations due to the mesh sensitivity test.

NOMECLATURE:

Symbol	Definition	Unite
D1	Inlet diameter of the impeller	mm
D2	Outlet diameter of impeller	mm
B1	Inlet blade width	mm
B2	Outlet blade width	mm
H	Head	mm
Q	Mass flow rate	Kg/s
Cu	Absolute tangential velocity	m/s
Cm	Absolute meridional velocity	m/s
r	Radius	mm
CD	drag coefficient	----
d	particle size, L, mm	mm
Di	impeller diameter, L, m	mm
GVF	inlet gas volumetric fraction	-----
h	channel height, L, mm	mm
H	hydraulic head, L, m	m
n	phase number	----
N	rotational speed, 1/L, rpm	RPM
NP	normalized pressure	Pa, N/m2

	increment	
ΔP	stage pressure increment,	Pa, N/m2
Q	volumetric flow rate,	M3/s
R	representative radius, L, mm	mm
RS	dimensionless notation	----
Re	Reynolds number	----
Sr	Strouhal number	----
v'	velocity fluctuation,	----
v	kinetic viscosity,	$N.s/m^2$
x	gas quality	
Y	height, L, m	mm
Z	blade number	----
b2	outlet width of impeller (mm)	mm
Cp	static pressure coefficient	----
D	diameter of impeller (mm)	mm
g	acceleration of gravity,	m/s^2
ns	specific speed	RPM
NPSHr	net positive suction head required (m)	m
R	radius of impeller (m)	m
RB	bubble radius	m

μt	turbulent viscosity	Pa·s
μeff	effective viscosity	Pa·s
Ω	rotational speed	RPM
φ	flow coefficient	----
ψ	head coefficient	----
ρ	fluid density,	kg/m^3
σ	surface tension,	N/m^2
ε	turbulent energy dissipation rate per unit mass, L2	m^2/s^3

ABBREVIATION:

Symbol	**Definition**
N	Blade count
t	Blade thickness
BEP	best efficiency point
b	bubble
B	blade
c	continuous phase
d	dispersed phase
D	diffuser or dispersed phase
G	gas phase
SR	slippage in the radial direction
VM	Notation

GREEK SYMBOLS:

Symbol	**Definition**	**Unite**
β1	Blade angle at the internal of an impeller	Degree
β2	Blade angle at the exit of the impeller	Degree
Θ	Wrap angle	Degree
η	Efficiency	-----
βm	The average vane angle Rotational speed	RPM
α	gas void fraction	----
λG	no-slip gas void fraction	----
μ	molecular viscosity,	$N.s/m^2$

References

1. Murakami, M. and Minemura, K."Effects of Entrained Air on the Performance of a Centrifugal Pump: 1st Report, Performance and Flow Conditions" *Bulletin of JSME* 1974, 17,110.
2. Pessoa, R. "Experimental investigation of two-phase flow performance of electrical submersible pump stages." *SPE Annual Technical Conference and Exhibition. OnePetro,* 2001.
3. Beltur, R. . "Experimental investigation of two-phase *flow performance of ESP stages.". PhD Thesis. the University of Tulsa* 2003 .
4. Barrios, L."Visualization and Modeling of Multiphase Performance inside an Electrical Submersible Pump". *PhD Thesis.The University of Tulsa,* 2007.
5. Mauricio, P. "Experimental Investigation of Two-Phase Flow Performance of Electrical Submersible Pump Stages" *SPE Annual Technical Conference and Exhibition. OnePetro,* 2001.

6. Salehi, E."ESP Performance in Two-Phase Flow through Mapping and Surging Tests at Various Rotational Speeds and Intake Pressures" *PhD Thesis. the University of Tulsa* 2012.
7. Schäfer, T., Bieberle, A., Neumann, M., and Hampel, U."Application of Gamma-ray Computed Tomography for the Analysis of Gas Holdup Distributions in Centrifugal Pumps" *Flow Measurement and Instrumentation*, 2015, 46: 262.
8. Furukawa, A., Shirasu, S., and Sato, S."Experiments on air-water two-phase flow pump impeller with rotating-stationary circular cascades and recirculating flow holes". *JSME International Journal Series B Fluids and Thermal Engineering*, 1996, 39.3: 575.
9. Barrios, L. and Prado, M. G."Experimental visualization of two-phase flow inside an electrical submersible pump stage" *Journal of Energy Resources Technology*, 2011, 133.4.
10. Bedrin, V. G., Khasanov, M. M., Khabibullin, R. A., Krasnov, V. A., Pashali, A. "High GLR ESP technologies comparison. Field test results" *Russian Oil and Gas Technical Conference, October* 28-30, 2008.
11. Pirouzpanah, S., Gudigopuram, S. R., & Morrison, G. L."Two-phase flow characterization in a split vane impeller Electrical Submersible Pump" *Journal of Petroleum Science and Engineering*, 2017, 148: 82.
12. M., Sagban.A "CFD Investigation of the Hydrodynamic Characteristics of Fluid Flow through an Impeller and Multi-Objective Design Optimization of a Centrifugal Pump" Master Thesis, Embry-Riddle Aeronautical University 2014.
13 "C & B Pumps & Compressors, LLC." 1997 http://www.candbsales.com.
14. "VistaTM CPD – centrifugal and mixed-flow pump preliminary design" 2009.
https://www.pcaeng.co.uk
15. "ANSYS, U.ANSYS TurboSystem User's Guide" 2013.
https://www.academia.edu/9518485/ANSYS_TurboSystem_Users_Guide.
16. "ANSYS, T.ANSYS TurboGrid User's Guide" 2016. https://pdfcoffee.com/ansys-turbogrid-users-guide-pdf-free.html.
17. "ANSYS CFX-Pre User's Guide" 2013.
https://www.pdfdrive.com/ansys-cfx-pre-users-guide-e12988705.html.
18. Rutvika, A."Investigation of Differences in Ansys Solvers CFX and Fluent" *Master Thesis, Royal Institute of Technology, KTH Stockholm* 2016.
19 "Orange ucdavis" 2017
. https://www.semanticscholar.org/paper/CFD-STUDY-OF-THE-DEVELOPMENT-OF-INTER-SUBCHANNEL-Wang/839a080422127368ad7075568df6a1b86e3e2b85.
20. Dawodu, "A.MODI-FIED DIOSCOREA ROTUNDATA PEEL CARBON : EQUILIBRIUM, KINETIC Petroleum and Coal Article".
Journal of Petroleum & Coal,(2018); 60(5): 985.
21. Bellary, S."Performance optimization of centrifugal pump for crude oil delivery" *The Journal of Engineering Research [TJER],* 2018, 15, 1, 88.
22. "ANSYS CFX-Solver Theory Guide" 2011.
.https://www.researchgate.net/publication/321628826_Study_on_Design_of_Pressure_Chamber_in_a_Linear-Jet_Type_Air_Curtain_System_for_Prevention_of_Smoke_Spread/fulltext/5a29ec470f7e9b63e5353c2d/Study-on-Design-of-Pressure-Chamber-in-a-Linear-Jet-Type-Air-Curtain-System-for-Prevention-of-Smoke-Spread.pdf.
23. " Heat and Mass Transfer Studies in Liquefied Petroleum Gas Storage Operations.". 2006.
https://core.ac.uk/download/pdf/11779223.pdf
24. Takacs, G."Electrical Submersible Pumps Manual: Design, Operations, and Maintenance,.Electrical submersible pump manual: design,operations, and maintenance". Book, Burlington, MA 01803, USA. 2009.
25. "pumping perfected. Gardner Denver." 2022.
. https://www.gdenergyproducts.com/
26. Van, E.Hydraulic performance of a mixed-flow pump: unsteady inviscid computations and loss models. *J. Fluids Eng.*, 2001, 123.2: 256.
27. "A CFD–PBM Coupled Model for Gas–Liquid Flows" 2005.
https://freepaper.me/PDF/?pdfURL=aHR0cHM6Ly9mcmVlcGFwZXIubWUvbi9vMWtOY1lSY25zQlBOOUJRV0p2dVFnL1BERi80Ny80N2UzZTRkYWZlOWYzYjMzNjkxZjBhMzNjNTkyYWRlNy5wZGY=&doi=10.1002/aic.10611.
28. "ANSYS CFX-Solver Theory Guide - ResearchGate." 2009.
file:///C:/Users/dell/Downloads/113AnsysCFXSolverTheoryGuide.pdf.